Available online at www.sciencedirect.com
SciVerse ScienceDirect
Journal of the European Ceramic Society xxx (2012) xxx–xxx
www.elsevier.com/locate/jeurceramsoc

Synthesis and sintering of YAG:Eu nanopowder

S.A. Hassanzadeh-Tabrizi

Department of Materials Engineering, Najafabad Branch, Islamic Azad University, Isfahan, Iran

Abstract

YAG:Eu nanopowder was synthesized through a sol–gel method. A master sintering curve was used as a practical approach to analyze the sintering behavior of the synthesized powder. The effect of MgO doping on sintering of the synthesized nanopowders was evaluated. An amorphous nanopowder was synthesized and crystallized to YAG after heat-treatment via a solid-state reaction. MgO improved the sintering rate of the YAG nanopowders and suppressed grain boundary mobility. The activation energy for sintering decreased from 917 to 837 kJ/mol by adding MgO to the nanopowders. The results of this study can be used to predict the densification of YAG:Eu nanopowder.

Keywords: Sol–gel processes; Sintering; Impurities; Microstructure-final; Nanopowder

1. Introduction

Yttrium aluminum garnet ($Y_3Al_5O_{12}$, YAG) is an important material because of its interesting optical properties. YAG doped with Ce, Sm, Tb, Eu and Cr shows excellent fluorescence properties.[1–3] Owing to such application potential of YAG ceramics, a lot of efforts have been made to try to synthesize YAG ceramics powders, such as sol–gel,[4] co-precipitation,[5] spray pyrolysis,[3] combustion,[6] solvo-thermal,[7] polyacrylamide gel.[8] Among these, the sol–gel method is a unique and useful method for obtaining well-dispersed YAG nanopowders with very good chemical homogeneity and high purity.

Sintering maps have been used to design and interpret sintering experiments, to better understand how changes in heating profiles affect sintering behavior, and to optimize sintering. A practical approach to predict and control sintering is based on the concept of the master sintering curve (MSC).[9–13] The MSC is an empirical curve that provides a characteristic measure of the densification of a material over a given density range. The MSC was originally developed and demonstrated for solid-state sintering materials that exhibit isotropic sintering behavior.[9] More recently, the master curve concept has been extended to systems that exhibit anisotropic sintering behavior, and that densify by liquid-phase and viscous-phase sintering.[9–13]

In this theory, $\Phi(\rho)$, a function of density, can be given as the function of temperature and time:

$$\Phi(\rho) = \theta(t, T(t)) = \int_{t_0}^{t} \frac{1}{T} \exp\left(-\frac{Q}{RT}\right) dt$$

where Q is the apparent activation energy for sintering, R is the gas constant, T is the absolute temperature, and t is the time. In this case, if the sintering process is dominated by only one diffusion mechanism (either volume or grain boundary diffusion) and the microstructure is a function of density, a MSC can be obtained.

In this study, YAG:Eu nanopowders were synthesized via a sol–gel method. The densification behavior is analyzed by master sintering curve concepts. As it is known, pores significantly degrade optical transparency of YAG ceramics and thus, using of dopants for improvement of densification in YAG ceramics is desirable. Therefore the effect of MgO on sintering of the YAG:Eu powders was studied.

2. Experimental procedure

The precursor solutions for YAG:Eu nanopowder were prepared by sol–gel method using $AlCl_3{\cdot}6H_2O$ (Merck), Al powder (Merck), Y_2O_3 (Aldrich), $EuCl_3{\cdot}6H_2O$ (Aldrich), sodium dodecyl sulfate (Aldrich) and HCl (Merck). The nominal composition was $(Y_{0.9}Eu_{0.1})_3Al_5O_{12}$. Y_2O_3 powder was first dissolved in aqueous HCl. The main solution was prepared by dissolving aluminum chloride hexahydrate, aluminum powder, europium chloride hexahydrate and yttrium oxide solution into the

E-mail addresses: hassanzadeh@pmt.iaun.ac.ir, tabrizi1980@gmail.com

0955-2219/$ – see front matter © 2012 Elsevier Ltd. All rights reserved.
doi:10.1016/j.jeurceramsoc.2012.02.046

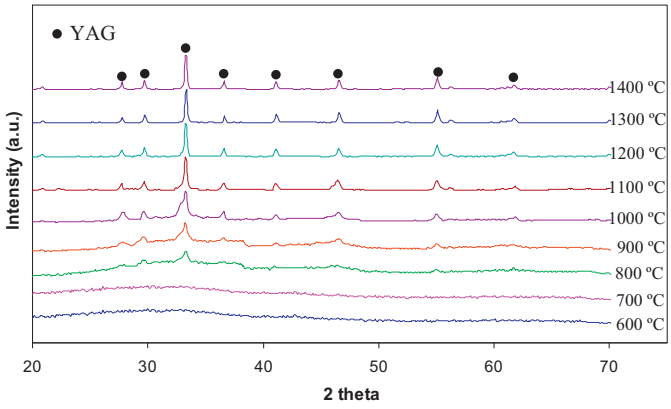

Fig. 1. The XRD patterns of samples heat treated at various temperatures for 3 h.

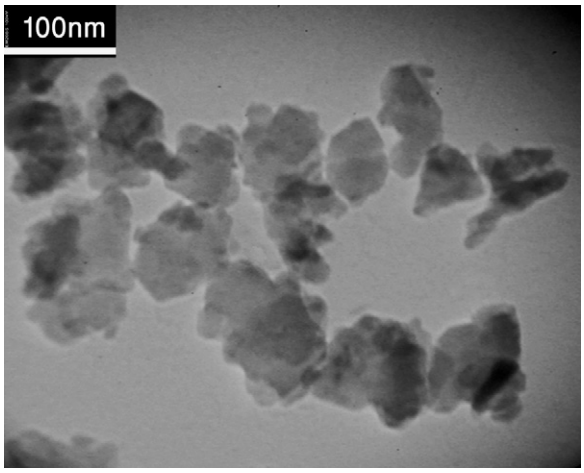

Fig. 2. TEM image of the nanopowders heat treated at 900 °C.

deionized water. The precursor solution was then continuously stirred at 100 °C for 4 h to completely dissolve the starting materials. SDS was added to the resultant sol. To study the effect of MgO on sintering behavior and microstructure of the YAG:Eu nanopowder, $MgCl_2{\cdot}6H_2O$ (Merck) was added to the precursor solution. The amount of MgO was 0.1 wt.%. The sol was aged at 60 °C. The viscosity of the batch gradually increased and finally the batch set to a rigid gel. It was then dried at 80 °C for 48 h. The dried gel was calcined in a muffle furnace at 900 °C and milled for 1 h in ethanol media using highly dense alumina jar and high-purity alumina balls. A ball to powder charge ratio of 5:1 (wt%) was used. The powders were cold isostatically pressed into compacts at the pressure of 400 MPa size 10 mm diameter 6 mm length. The samples were sintered in air using a dilatometer to construct the master sintering curve. For non-isothermal sintering, two heating rates of 2 °C/min and 5 °C/min were used to reach the maximum temperature without holding. Dilatometric data were used to determine the density (ρ) applying the following equation:

$$\rho = \left[\frac{1}{1-(dL/L_0)+\alpha(T-T_0)}\right]^3 \rho_g$$

where dL/L_0 is instantaneous linear shrinkage, L_0 is the initial length of compact, α is the coefficient of thermal expansion and ρ_g is the green density.

The crystalline structure of the powders was determined by X-ray diffraction using a Philips X-pert model with Cu Ka radiation. The microstructure of the samples was observed by scanning electron microscopy (SEM, XL30-Phillips, Netherlands) and transmission electron microscopy (TEM, CM200-FEG-Phillips, Netherlands).

3. Results and discussion

The X-ray diffraction patterns of the gel heat-treated for 3 h at temperature ranges from 600 to 1400 °C are shown in Fig. 1. There are no diffraction peaks for the samples calcined up to 700 °C indicating that the powders are amorphous below this temperature. The characteristic peaks of YAG phase appear at 800 °C and no other crystalline phase such as $Y_4Al_{12}O_9$ (YAM) or $YAlO_3$ (YAP) can be detected. The crystallization temperature of YAG powder prepared by the sol–gel method is lower than that in the solid-state reaction by the constituent oxide mixtures.[14]

Fig. 2 shows the TEM image of the nanopowders heat treated at 900 °C. As can be seen a uniform structure consisting of irregular particles with sizes up to 120 nm. There are some agglomerates in the powders. During the drying step, the particles form agglomerates due to their high adhesion activity after the evaporation of water.[15]

Fig. 3 shows dilatometric curves of the YAG:Eu (Fig. 3a) and MgO doped YAG:Eu (Fig. 3b) samples. All specimens showed an isotropic shrinkage behavior. The sample doped with MgO exhibits higher percentage of shrinkage than undoped sample. The temperature for densification onset for the doped sample was lower than the pure sample. More shrinkage was obtained when the heating rate was 2 °C/min, because the samples are exposed to sintering for a longer time. In addition Bernard-Granger and Guizard[16] explained that surface diffusion is assisting densification for low heating rates values. This kind of "boost effect", given by surface diffusion to densification until the neck formation step is completed, enables attaining higher relative densities at the end of firing when heating rate is low.

Fig. 4 shows the relative density for the samples as a function of temperature when the heating rate was 2 °C/min. It can be seen that, the densification improved by doping the samples with MgO. At the same heating rate, doped sample starts to densify at a lower temperature, and a significantly lower temperature is required to achieve the end-point density. Adding of MgO can result in a solid solution formation by substitution of Al^{3+} by Mg^{2+} as follows:

$$2MgO \xrightarrow{Al_2O_3} 2Mg'_{Al} + V_O^{\bullet\bullet} + 2O_O$$

According to this equation, one expects that the formation of oxygen vacancies improves the volume diffusion coefficient and could precede the vacancies diffuse from the pore to the grain boundaries. The vacancies are eliminated at the grain boundaries, can cause an increase in densification rate. In this work, the samples were not reached to full density. This problem can be alleviated by sintering in a vacuum. As it is known sintering

Please cite this article in press as: Hassanzadeh-Tabrizi SA. Synthesis and sintering of YAG:Eu nanopowder. *J. Eur. Ceram. Soc.* (2012), doi:10.1016/j.jeurceramsoc.2012.02.046

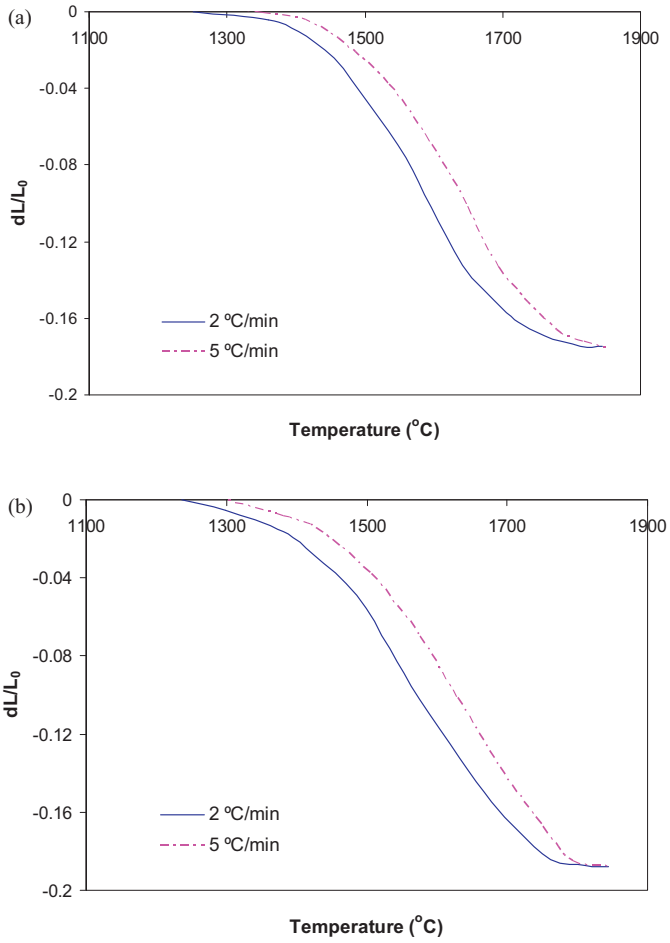

Fig. 3. Dilatometric curves of the (a) pure YAG:Eu and (b) MgO doped YAG:Eu samples.

in a gaseous atmosphere leads to trapped gases in the pores, so densification stops when the increasing gas pressure in the shrinking pores equals the sintering stress, resulting in a limiting final density.[17] In addition, the existence of agglomerates has a negative effect on the increase of density. It was found that, dry

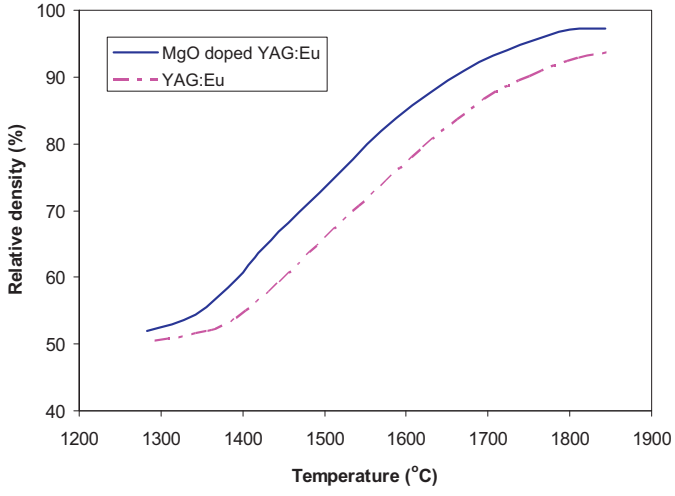

Fig. 4. The relative density of the samples as a function of temperature when the heating rate was 2 °C/min.

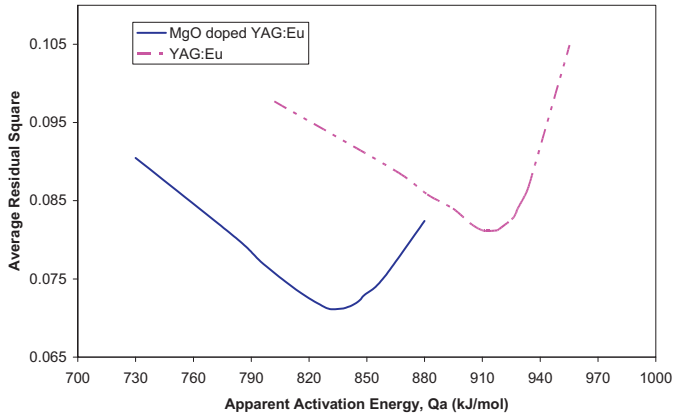

Fig. 5. Mean residual squares of error for various values of the activation energy.

pressing of the agglomerated nanopowders leads to a green body microstructure with two types of pores: interagglomerate pores with micrometric scales that coexist with smaller intercrystallite pores with nanometric scales within the agglomerates.[18] During the sintering process, intercrystallite pores shrink but the interagglomerate pores remain in the microstructure.

For the construction of the MSC, the value of activation energy (Q) should be determined first.[19] The apparent activation energy for the MSC is determined by minimizing the mean

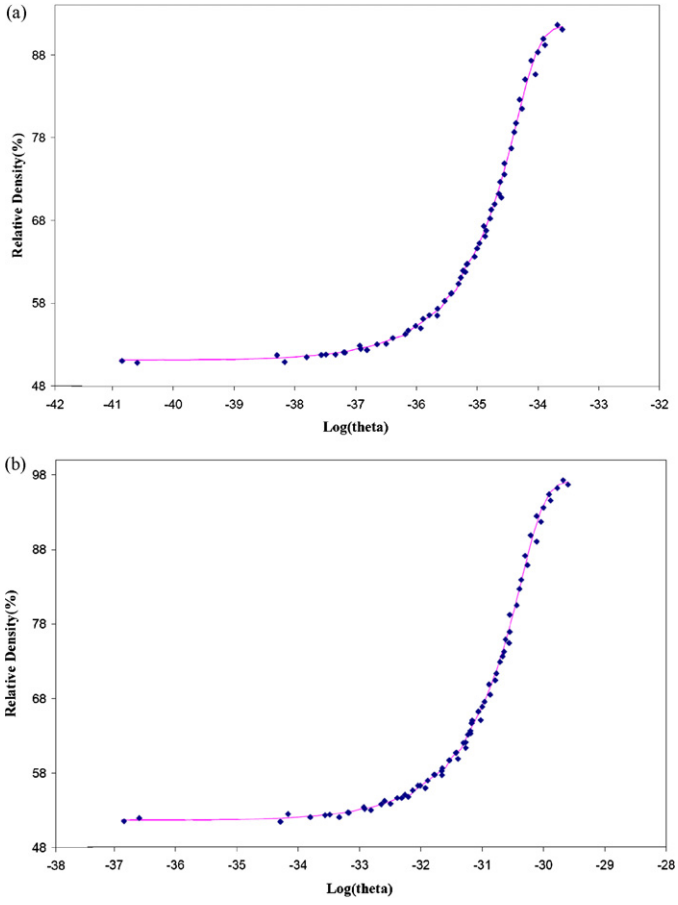

Fig. 6. Master sintering curves for (a) pure YAG:Eu and (b) MgO doped YAG:Eu powder compacts.

Please cite this article in press as: Hassanzadeh-Tabrizi SA. Synthesis and sintering of YAG:Eu nanopowder. *J. Eur. Ceram. Soc.* (2012), doi:10.1016/j.jeurceramsoc.2012.02.046

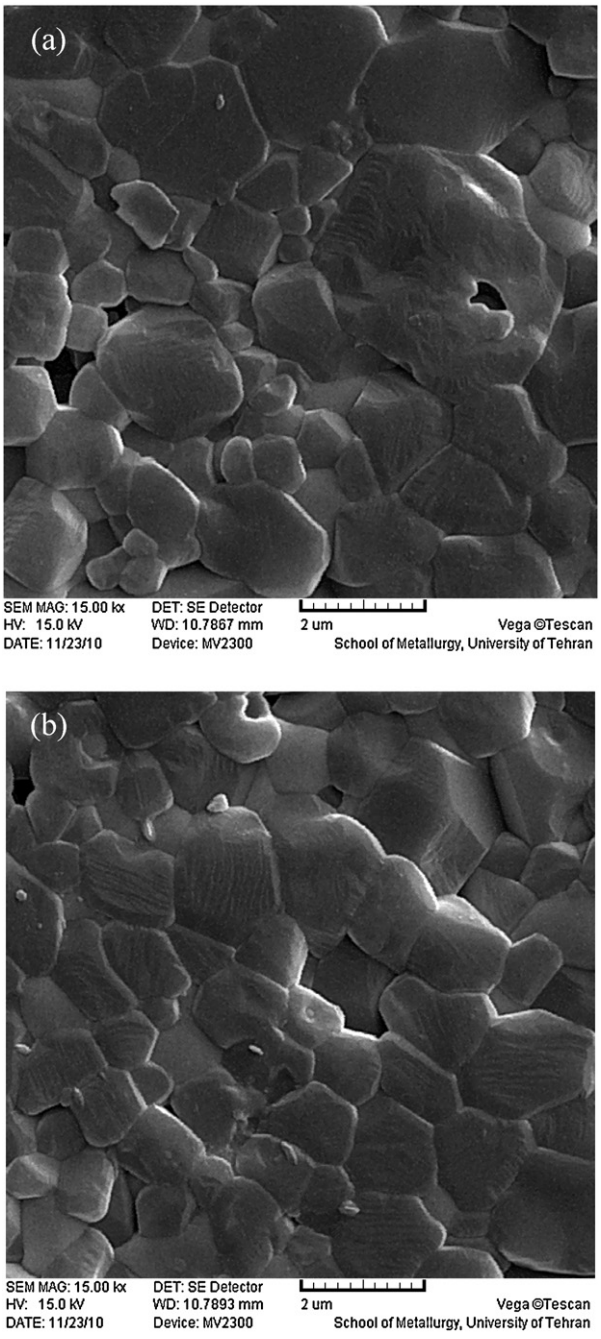

Fig. 7. The SEM images of the (a) pure YAG:Eu and (b) MgO doped YAG:Eu specimens sintered at 1750 °C for 3 h.

residual squares of error.[20] For this purpose, an estimation was taken as starting value for the activation energy Q, and the related MSC including all three heating profiles was constructed. By the optimum of Q, all curves should converge. If the curves did not converge then another value for Q was taken and the procedure continued until the best estimate of Q was obtained (Fig. 5). The apparent activation energy values for the whole sintering behavior obtained on this basis for the pure and doped samples were 917 and 837 kJ/mol, respectively. It is clear that adding MgO can cause reduction in activation energy for sintering of YAG:Eu, which may be used to explain why MgO doping leads to a decrease in sintering temperature.

The MSC curves can now be constructed from the complete set of experimental data for the samples (Fig. 6). Almost all of the sintering data for the pressed powder compacts sintered at 2 and 5 °C/min collapsed onto a single master curve. A good fit of the data to the MSC is an indication of a good Q value. Su and Johnson[9] noted that the MSC applies only to green powder compacts processed with the same powder to the same green density using the same green forming process. The grain growth at higher densities will shift the higher density part of the MSC down and to the right. MgO doping results in a lower value of $\theta(t,T(t))$ at a given density than the pure sample.

Fig. 7 presents the SEM images of the specimens sintered at 1750 °C for 3 h. The grains are fairly equiaxed in shape, without any observable abnormal or anisotropic grain growth. It can be seen that a small amount of MgO doping decreases the grain size of the samples. MgO is segregated as solute at the grain boundaries where it then exerts a drag on grain-boundary motion.[21] The segregation of solute causes a decrease in the grain-boundary mobility, and then inhibits the grain growth.

4. Conclusion

In the present study a YAG:Eu nanopowder was synthesized through a modified aqueous sol–gel method. Master sintering curve theory has been applied successfully to the sintering of YAG:Eu nanopowder compacts. An amorphous nanopowder was prepared and it was crystallized to YAG after heat-treatment via a solid state reaction. The results showed that a systematic approach to design and control YAG:Eu nanopowder sintering is possible through the implementation of the MSC. Small amount of MgO doping enhanced the densification rate and suppressed the grain growth of the YAG nanopowder. The activation energy for sintering decreased from 917 to 837 kJ/mol by adding MgO to the nanopowders.

References

1. Sim SM, Keller KA. Phase formation in yttrium aluminum garnet powders synthesized by chemical methods. *J Mater Sci* 2000;**35**:713–7.
2. Zhang XD, Liu H, He W, Wang JY, Li X, Boughton RI. Synthesis of monodisperse and spherical YAG nanopowder by a mixed solvothermal method. *J Alloys Compd* 2004;**372**:300–3.
3. Zhou YH, Lin J, Yu M, Han SM, Wang SB, Zhang HJ. Morphology control and luminescence properties of YAG:Eu phosphors prepared by spray pyrolysis. *Mater Res Bull* 2003;**38**:1289–99.
4. Fujioka K, Saiki T, Motokoshi S, Fujimoto Y, Fujita H, Nakatsuk M. Luminescence properties of highly Cr co-doped Nd:YAG powder produced by sol–gel method. *J Lumin* 2010;**130**:455–9.
5. Su J, Zhang QL, Shao SF, Liu WP, Wan SM, Yin ST. Phase transition, structure and luminescence of Eu:YAG nanophosphors by co-precipitation method. *J Alloys Compd* 2009;**470**:306–10.
6. Yen-Pei F, Shaw-Bing W, Chin-Shang H. Preparation and characterization of $Y_3Al_5O_{12}$:Ce and Y_2O_3:Eu phosphors powders by combustion process. *J Alloys Compd* 2008;**458**:318–22.
7. Wu Z, Zhang X, He W, Du Y, Jia N, Xu G. Preparation of YAG:Ce spheroidal phase-pure particles by solvo-thermal method and their photoluminescence. *J Alloys Compd* 2009;**468**:571–4.

Please cite this article in press as: Hassanzadeh-Tabrizi SA. Synthesis and sintering of YAG:Eu nanopowder. *J. Eur. Ceram. Soc.* (2012), doi:10.1016/j.jeurceramsoc.2012.02.046

8. Chun-jia L, Rui-min W, Zhi-wei X, Jing C, Xing-huang Y, Xue-tao L. Crystallization, morphology and luminescent properties of YAG:Ce^{3+} phosphor powder prepared by polyacrylamide gel method. *Trans Nonferrous Met Soc China* 2007;**17**:1093–9.
9. Su H, Johnson DL. Master sintering curve, a practical approach to sintering. *J Am Ceram Soc* 1996;**79**:3211–7.
10. Sethi G, Park SJ, Johnson JL, German RM. Linking homogenization and densification in W–Ni–Cu alloys through master sintering curve (MSC) concepts. *Int J Refract Met Hard Mater* 2009;**27**:688–95.
11. Ewsuk KG, Ellerby DT. Analysis of nanocrystalline and microcrystalline ZnO sintering using master sintering curves. *J Am Ceram Soc* 2006;**89**:2003–9.
12. Pouchly V, Maca K. Master sintering curve – a practical approach to its construction. *Sci Sinter* 2010;**42**:25–32.
13. Kiani S, Pan J, Yeomans JA. A new scheme of finding the master sintering curve. *J Am Ceram Soc* 2006;**89**:3393–6.
14. Yada M, Ohya M, Machida M, Kima T. Synthesis of porous yttrium aluminium oxide templated by dodecyl sulfate assemblies. *Chem Commun* 1998;**18**:1941–2.
15. Kwon S, Messing GL. The effect of particle solubility on the strength of nanocrystalline agglomerates: boehmite. *Nanostruct Mater* 1997;**8**:399–418.
16. Bernard-Granger G, Guizard C. Apparent activation energy for the densification of a commercially available granulated zirconia powder. *J Am Ceram Soc* 2007;**90**:1246–50.
17. Rahaman MN. *Ceramic. Processing and Sintering*. 2nd ed. New York: Marcel Dekker; 2003.
18. Bowen P, Carry C. From powders to sintered pieces: forming, transformations and sintering of nanostructured ceramic oxides. *J Powder Technol* 2002;**128**:248–55.
19. Hanson J, Rusin RP, Teng M, Johnson DL. Combined-stage sintering model. *J Am Ceram Soc* 1992;**75**:1129–35.
20. Li D, Chen S, Shao W, Ge X, Zhang Y, Zhang S. Densification evolution of TiO_2 ceramics during sintering based on the master sintering curve theory. *Mater Lett* 2008;**62**:849–51.
21. Jorgensen PJ, Westbrook JH. Role of solute segregation at grain boundaries during final-stage sintering of alumina. *J Am Ceram Soc* 1964;**47**:332–8.

Please cite this article in press as: Hassanzadeh-Tabrizi SA. Synthesis and sintering of YAG:Eu nanopowder. *J. Eur. Ceram. Soc.* (2012), doi:10.1016/j.jeurceramsoc.2012.02.046